Proc. Natl. Acad. Sci. USA
Vol. 96, pp. 9539–9544, August 1999
Biochemistry

Rapid GTP binding and hydrolysis by G_q promoted by receptor and GTPase-activating proteins

SUCHETANA MUKHOPADHYAY AND ELLIOTT M. ROSS*

Department of Pharmacology, University of Texas Southwestern Medical Center, 5323 Harry Hines Boulevard, Dallas, TX 75235-9041

Communicated by Eva J. Neer, Harvard Medical School, Boston, MA, June 23, 1999 (received for review May 11, 1999)

ABSTRACT **Receptor-promoted GTP binding and GTPase-activating protein (GAP)-promoted GTP hydrolysis determine the onset and termination of G protein signaling; they coordinately control signal amplitude. The mechanisms whereby cells independently regulate signal kinetics and signal amplitude are therefore central to understanding G protein function. We have used quench-flow kinetic methods to measure the rates of the individual reactions of the agonist-stimulated GTPase cycle for G_q during steady-state signaling. G_q and m1 muscarinic cholinergic receptor were co-reconstituted into proteoliposomes with one of two GAPs: phospholipase C (PLC)-β1, the major G_q-regulated effector protein, and RGS4, a GAP commonly thought to be an inhibitor of G_q signaling. In this system, the rate constant for GAP-stimulated hydrolysis of $G\alpha_q$-bound GTP at 30°C was 9–12 s^{-1} for PLC-β1 and 22–27 s^{-1} for RGS4. These rates are 1,000- to 2,000-fold faster than in the absence of a GAP and far faster than measured previously. G_q can thus hydrolyze bound GTP with deactivation half-times of 25–75 ms at 30°C, commensurate with physiological rates of signal termination. GDP/GTP exchange, which reactivates G_q, was the principal rate-limiting step for the GTPase cycle and was also faster than previously thought. At physiological concentrations of GTP, exchange was limited by the rate of dissociation of GDP from the receptor–G_q complex, with a maximal rate of 1.8 s^{-1} at 30°C. Comparison of activation and deactivation rates help explain how GDP/GTP exchange balance rapid GTP hydrolysis to maintain steady-state signal amplitude.**

The initiation, amplitude, and termination of G protein signaling are all determined by a tightly controlled cycle of activation and deactivation. GTP binding, the activation step, is promoted by G protein-coupled receptors; hydrolysis of bound GTP, and consequent deactivation is accelerated by GTPase-activating proteins (GAPs). GAPs perform two fundamentally different functions in G protein signaling. First, a GAP can simply inhibit signaling by decreasing the fraction of G protein that is in the active state during the GTPase cycle. Several GAPs function physiologically as signaling inhibitors (1–3), and overexpression of GAPs can inhibit G protein pathways in many cells [reviewed in (4–6)]. Alternatively, GAPs can accelerate signal termination on removal of agonist without substantially inhibiting steady-state signaling. GAPs thereby enhance the temporal acuity of the signaling process without attenuating the signal itself (4, 7). For example, expression of two G_i GAPs, RGS4 or RGS8, accelerated potassium channel deactivation on agonist removal more than 20-fold but caused little if any decrease in net conductance during agonist stimulation (8–11). How GAP-stimulated deactivation is balanced with receptor-promoted activation to give rapid turn-off with minimal inhibition of signal amplitude is not well understood mechanistically.

G protein GAPs include two functional groups of proteins, effectors and regulator of G protein signaling (RGS) proteins, whose GAP activities are commonly thought to fulfill different purposes. The first G protein GAP to be identified was phospholipase C (PLC)-β1, which is both the principal G_q-regulated effector and an active, G_q-specific GAP (12). Similarly, p115 rhoGEF is both a G_{13} GAP and a G_{13}-regulated effector protein (13, 14), and type V adenylyl cyclase has recently been reported to have G_s GAP activity (15). The physiological function of GAP activity in an effector protein is not well understood, but it is clearly important in allowing rapid termination of downstream signaling when agonist is removed. Without such GAP activity, the decay of G protein signaling on termination of input from receptor would take up to 10 s at physiological temperatures, far longer than usually observed physiologically and much too slow for many signaling events (synaptic transmission, response to light, secretion, contraction, etc.) (4, 7, 16).

RGS proteins, which are GAPs for the G_i and G_q families, are not known to act as G protein-regulated effectors and are commonly assumed to be inhibitors of G protein signaling (5, 6). An exception to this assumption is RGS9, the major RGS protein in mammalian retinal photoreceptor cells, whose principal physiological function is thought to be the rapid deactivation of G_t after illumination (7, 17). The GAP activity of RGS9 is potentiated by the γ subunit of cGMP phosphodiesterase, the G_t effector, and its GAP activity may be more analogous to that of the effectors mentioned above (17).

Regardless of their precise physiological functions, the steady-state inhibitory potential of a GAP must be reconciled with its role in sharpening the turn-off process when stimulation ends. If GAP activity is to be used for rapid signal termination without squelching the signal, then rapid GTP hydrolysis must be balanced by commensurately fast activation by GTP binding. Intuitively, this balance is necessary for those effectors that are also GAPs. To explain the potential conflict of rapid turn-off and high steady-state signal output, we proposed that fast GTP hydrolysis allows receptors to remain bound to G proteins throughout the GTPase cycle and thereby catalyze reactivation more efficiently (18). This stable receptor–G protein–GAP complex would turn over GTP rapidly, but the receptor would be able to keep up with the activity of the GAP.

To evaluate the interactive effects of receptors and GAPs on G protein signaling, we have used quench-flow mixing to study the individual steps in the GTPase cycle in reconstituted phospholipid vesicles that contain G_q and m1 muscarinic cholinergic receptor (m1AChR). We found that PLC-β1 accelerates the hydrolysis of G_q-bound GTP >1,000-fold and that RGS4 can accelerate hydrolysis >2,000-fold. The lifetime of the G_q–GTP complex under these conditions is 25–75 ms,

The publication costs of this article were defrayed in part by page charge payment. This article must therefore be hereby marked "*advertisement*" in accordance with 18 U.S.C. §1734 solely to indicate this fact.

PNAS is available online at www.pnas.org.

Abbreviations used: GAP, GTPase activating protein; GTPγS, guanosine 5′-[γ-thio]triphosphate; PLC-β1, phospholipase C-β1; m1AChR, m1 muscarinic cholinergic receptor; RGS, regulator of G protein signaling.

*To whom reprint requests should be addressed. E-mail ross@utsw.swmed.edu.

well within the range of physiological turn-off rates. To accommodate such rapid hydrolysis, receptor-catalyzed GDP release achieved a rate of 1.8 s^{-1}. These data indicate that heterotrimeric G proteins can hydrolyze GTP rapidly and that the hydrolysis rate is matched by receptor-catalyzed GDP/GTP exchange.

EXPERIMENTAL PROCEDURES

Materials. [^{35}S]guanosine 5′-[γ-thio]triphosphate ([^{35}S]GTPγS), [γ-^{32}P]GTP, and [α-^{32}P]GTP were purchased from NEN. [γ-^{32}P]GTP was further purified, and [α-^{32}P]GDP was synthesized and purified as described (18). Sources of all other reagents have been described (18, 19). Wild-type m1AChR, $G\alpha_q$, and $G\beta_1\gamma_2$, and hexahistidine-tagged PLC-β1 were expressed in Sf9 cells and purified as described (18). Hexahistidine-tagged RGS4 was expressed in *Escherichia coli* and purified as described (20).

m1AChR-G_q Proteoliposomes. m1AChR and G_q were coreconstituted into unilamellar phospholipid vesicles (phosphatidylethanolamine/phosphatidylserine/cholesteryl hemisuccinate, 165:98:18) as described (18). The concentration of m1AChR in the vesicles was measured by [^{3}H]quinuclidinyl benzilate binding (19). Receptor-coupled $G\alpha_q$ was measured as carbachol-stimulated [^{35}S]GTPγS binding as described (19). To minimize background, receptor-coupled $G\alpha_q$ assays were routinely performed at 0.4 μM [^{35}S]GTPγS, which may underestimate receptor-coupled $G\alpha_q$ by as much as 50%. Thus, values of $k_{cat} = V_{max}/[E]$ for steady-state GTPase may be overestimated up to 2-fold, and the amounts of binding or hydrolysis in pre-steady-state bursts often appear to be just above the "total" amount of coupled G_q.

Steady-State GTPase Assays. In all experiments, m1AChR-G_q vesicles and GAP, when present, were preincubated in assay buffer (20 mM Hepes/0.1 M NaCl/2 mM $MgCl_2$/1 mM EGTA/0.1 mg/ml BSA/1 mM DTT) with either 1 mM carbachol or 10 μM atropine for 3 min at 30°C or 15 min at 10°C. The same assay buffer was also used in all presteady-state experiments described below except as noted. Assays were initiated by addition of [γ-^{32}P]GTP at concentrations shown in the figure legends. Assay times were adjusted to ensure linear reactions according to the GTPase activities and the concentration of substrate. Reactions were quenched with a slurry of cold 5% Norit in H_3PO_4 (pH 3.0), and [^{32}P]P_i was measured in the supernatant as described (18).

Determination of Intermediary Reaction Rates During Steady-State GTP Hydrolysis. To measure the kinetics of the individual reactions that make up the GTPase catalytic cycle (Scheme I), the complete reaction mixture (m1AChR-G_q vesicles, GAP, agonist, GTP) was first allowed to reach steady state. Radiolabeled nucleotide was then added, and the reaction was terminated at different stages to monitor hydrolysis of $G\alpha_q$-bound GTP (k_{hydrol}), GDP dissociation (k_{diss}), or GDP/GTP exchange (k_{exch}). [We define k_{exch} as the observed first-order rate constant for the binding of GTP (or GTPγS) to G_q. It is a combined measure of GDP release and GTP binding.] Because most partial reactions are relatively rapid, assays were usually performed by using a Bio-Logic SFM4/Q four-syringe, quench-flow mixer in which Kel-F syringes, mixing chambers, and delay lines are all under thermostat control. Syringe movement is independently computer-controlled by using stepper motors to drive the plungers. In typical experiments, syringe 1 contained assay buffer that was used to drive reagents through the system as they were mixed. Reaction mixtures were expelled into a final cold quenching solution at 0°C as the final step in each experiment. The external quench was complete in ≤17 ms as determined by time-lapse video recording of the mixing of neutral-pH mock assay volumes that were ejected into acidic solutions of pH-sensitive dyes (data not shown). Quench-flow experimental protocols were designed to minimize the required amount of enzyme, background reactions, and cross-contamination among syringes and to maximize recovery of reactants, signal/background ratio, and final radioisotope signal. We describe all quench-flow experiments in terms of the volume of final reaction mixture that was collected and analyzed for product (bound nucleotide or [^{32}P]P_i). We ignore excesses needed to provide leading and trailing volumes of reactants whose concentrations were critical or reagents used to flush mixers and the delay lines before reactions. Detailed mixing protocols are available from the authors. Control experiments indicated that dead times were significantly shorter than any incubation time and that negligible protein denaturation occurred during incubation of vesicles in the syringe and/or during high-speed flow through the mixing apparatus (data not shown). Some slower reactions were measured manually, as noted in the text.

Hydrolysis of G_q-Bound GTP. To measure the rate of hydrolysis of G_q-bound GTP during steady-state turnover, m1AChR-G_q vesicles, GAP, and agonist were first mixed to allow association of receptor and G_q (18). Vesicles and either 44 nM PLC or 9 μM RGS4 were incubated with 1 mM carbachol in a syringe of the quench-flow mixer for ≥15 min at 10°C or ≥3 min at 30°C. An aliquot (20 μl) was diluted 1:2 with assay buffer that contained carbachol and [γ-^{32}P]GTP (300–700 nM), and the mixture was incubated for 1 min (10°C) or 6 s (30°C) to initiate steady-state hydrolysis and allow accumulation of G_q–[γ-^{32}P]GTP without excessive production of background [^{32}P]P_i. At this point, defined as $t = 0$, further [γ-^{32}P]GTP binding was quenched by 1:1.5 dilution with 100 μM nonradioactive GTP and 100 μM atropine in assay buffer (to inhibit dissociation of bound [γ-^{32}P]GTP). This reaction mixture was incubated for the times shown and then quenched by mixing with 1.8 vol of 5% Norit charcoal in 50 mM H_3PO_4 (pH 3.0) at 0°C. ^{32}P-Labeled orthophosphate was monitored as described (19). Zero-time background radioactivity was subtracted from all data. For this and other assays of reaction transients, data were fitted to single or double exponential equations (SIGMAPLOT, SPSS, Chicago).

Receptor-Stimulated GDP Dissociation. [α-^{32}P]GDP was first bound to reconstituted G_q by incubating m1AChR-G_q vesicles, 1 mM carbachol, and 300 nM [α-^{32}P]GDP (70–100 cpm/fmol) in a syringe of the quench-flow mixer for at least 15 min at 10°C or 5 min at 30°C. Aliquots of this mixture (30 μl) were diluted 1:2 with agonist and 0.3–500 μM unlabeled GTP at $t = 0$, and the dissociation reaction was allowed to proceed for various times. The reaction was quenched in cold buffer that contained detergent and atropine (18), and the amount of G_q-bound [α-^{32}P]GDP was measured by nitrocellulose filter binding (21). Identical results were obtained when [α-^{32}P]GDP was bound to G_q in the presence of a GAP.

$$\text{R-G}\alpha + \text{GTP} \underset{}{\overset{k_{assoc}}{\rightleftharpoons}} \text{R-G}\alpha\text{–GTP} \xrightarrow{k_{hydrol}} \text{R-G}\alpha\text{-GDP + Pi} \overset{k_{diss}}{\rightleftharpoons} \text{R-G}\alpha + \text{GDP}$$

Guanine Nucleotide Exchange. Rates of receptor-catalyzed nucleotide exchange on G_q were measured by first equilibrating vesicles and agonist and then initiating exchange by the addition of radiolabeled nucleotide. m1AChR-G_q vesicles (30 μl) were first incubated in assay buffer plus 1 mM carbachol, either alone or with 44 nM PLC-β1 or 7 μM RGS4. Exchange reactions were initiated by 1:2 dilution of vesicles with [α-^{32}P]GTP, [α-^{32}P]GDP, or [^{35}S]GTPγS plus carbachol. Final concentrations of nucleotides are indicated in the legends. Reactions were quenched by adding 100 μl of cold stop buffer

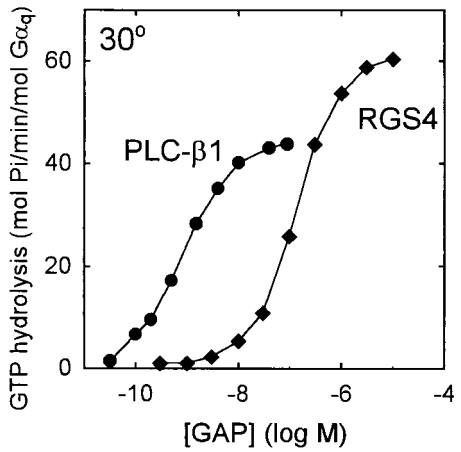

FIG. 1. GAP activity of PLC-β1 and RGS4 during steady-state GTP hydrolysis. The carbachol-stimulated GTPase activity of proteoliposomes that contained m1AChR and G_q was assayed at 30°C in the presence of increasing concentrations of PLC-β1 (●) or RGS4 (♦). Vesicles were preincubated with 1 mM carbachol and either GAP for 3 min before addition of 10 μM [γ-^{32}P]GTP to initiate the reaction. Data shown are representative of several complete titration curves (n = 2 for PLC-β1, n = 3 for RGS4) and multiple other experiments.

(GTP, atropine, detergent; ref. 18), and bound nucleotide was measured by nitrocellulose filter binding (21).

RESULTS

Steady-State G_q GAP Activities of PLC-β1 and RGS4. Both PLC-β1 and RGS4 stimulated the steady-state GTPase activity of m1AChR-G_q vesicles from the basal rate of 0.8–1.0 mol of GTP·min^{-1}·mol^{-1} of Gα_q to over 40 mol of GTP hydrolyzed·min^{-1}·mol^{-1} of G_q (Fig. 1). PLC-β1 typically increased activity >20-fold, although 60-fold stimulations have been observed (18) (confirmed in this study). RGS4 usually stimulated GTPase activity to a maximum 1.5- to 2.5-fold greater than that of PLC-β1, although its EC_{50}, 200–300 nM, is well above the 2 nM EC_{50} of PLC-β1. Different preparations of vesicles with m1AChR/G_q ratios of 0.1–0.3 yielded consistent EC_{50} values for both GAPs, but maximum turnover numbers increased up to 2-fold with increasing receptor/G_q ratios. Both PLC-β1 and RGS4 increased the K_m of the receptor-G_q vesicles from about 100 nM GTP to 1–3 μM GTP (Fig. 2). The elevated K_m accompanied by the large increase in V_{max} suggests that both GAPs accelerate steady-state hydrolysis primarily or exclusively by increasing the rate of hydrolysis of G_q-bound GTP. None of the parameters shown in Fig. 1 except for V_{max} were substantially different at 10°C or 30°C.

PLC-β and RGS4 Accelerate Hydrolysis of G_q-Bound GTP 1,000- to 2,000-Fold. To measure the effect of GAPs on the rate of hydrolysis of G_q-bound GTP during the steady-state GTPase cycle (k_{hydrol}), we allowed agonist-liganded receptor and G_q to associate in the vesicles (18), added [γ-^{32}P]GTP for a brief period to allow it to bind to G_q, and then quenched further binding with excess unlabeled GTP. We then monitored release of [^{32}P]P_i from the preformed pool of G_q–[γ-^{32}P]GTP (Fig. 3). A substantial fast and monoexponential burst of [^{32}P]P_i release occurred in the presence of either PLC-β1 or RGS4. At 30°C, values of k_{hydrol} in the burst phase were 9–12 s^{-1} for PLC-β1 and 22–27 s^{-1} for RGS4 (12 s^{-1} and 27 s^{-1} in Fig. 3). This maximum rate is >2,000-fold faster than the basal value of k_{hydrol} previously measured for G_q, 0.013 s^{-1} (12), confirmed in this study, and corresponds to a $t_{1/2}$ of 25–75 ms for the deactivation of G_q by GTP hydrolysis. The relative difference in k_{hydrol} between PLC-β1 and RGS4 is about equal to the difference in their abilities to stimulate steady-state hydrolysis (Fig. 2). At 10°C, hydrolysis of Gα_q-GTP was substantially slower. PLC-β1 and RGS4 increased k_{hydrol} from 0.0019 s^{-1} to 0.8–0.9 s^{-1} and 1.2–1.6 s^{-1}, respectively. We have not tried to measure the hydrolysis of G_q–GTP at 37°C, but we estimate from the data described above that the rate of GAP-stimulated hydrolysis would be about 25 and 65 s^{-1} for PLC-β1 and RGS4, yielding deactivation half-times of about 30 ms and 10 ms, respectively. These are well within the deactivation lifetimes reported for G protein signaling pathways *in vivo*, suggesting that GAP-stimulated GTP hydrolysis can fully account for the termination of signaling on removal of receptor agonist.

The burst of G_q–[γ-^{32}P]GTP hydrolysis was only observed in vesicles where the m1AChR/G_q molar ratio was at least 0.3. The amount of [^{32}P]P_i released in the burst was reproducible for each batch of vesicles. The magnitude of the burst increased with the concentration of [γ-^{32}P]GTP in the binding reaction in a pattern consistent with the K_m for steady-state GTPase

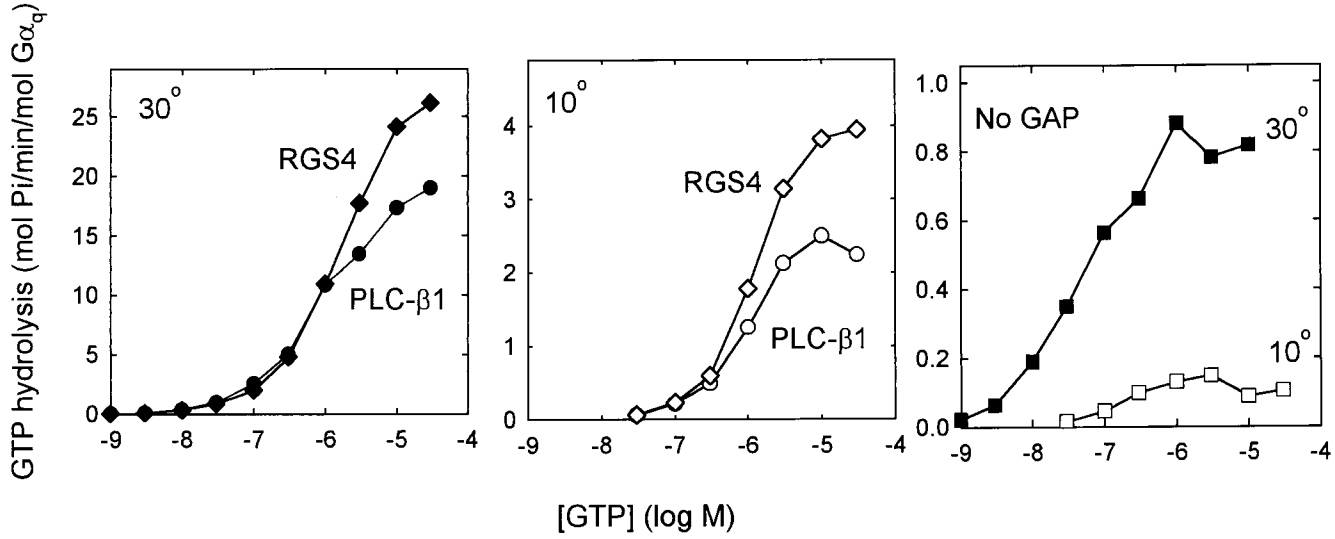

FIG. 2. Dependence of agonist-stimulated steady-state GTPase activity on GTP concentration. The carbachol-stimulated GTPase activity of m1AChR-G_q vesicles was assayed with either 15 nM PLC-β1 or 4 μM RGS4 in the presence of increasing concentrations of GTP. (*Left*) 30°C, PLC-β1 (●) or RGS4 (♦). (*Center*) 10°C, PLC-β1 (○) or RGS4 (◇). (*Right*) No GAP, 30°C (■) or 10°C (□). Data are means from two separate experiments.

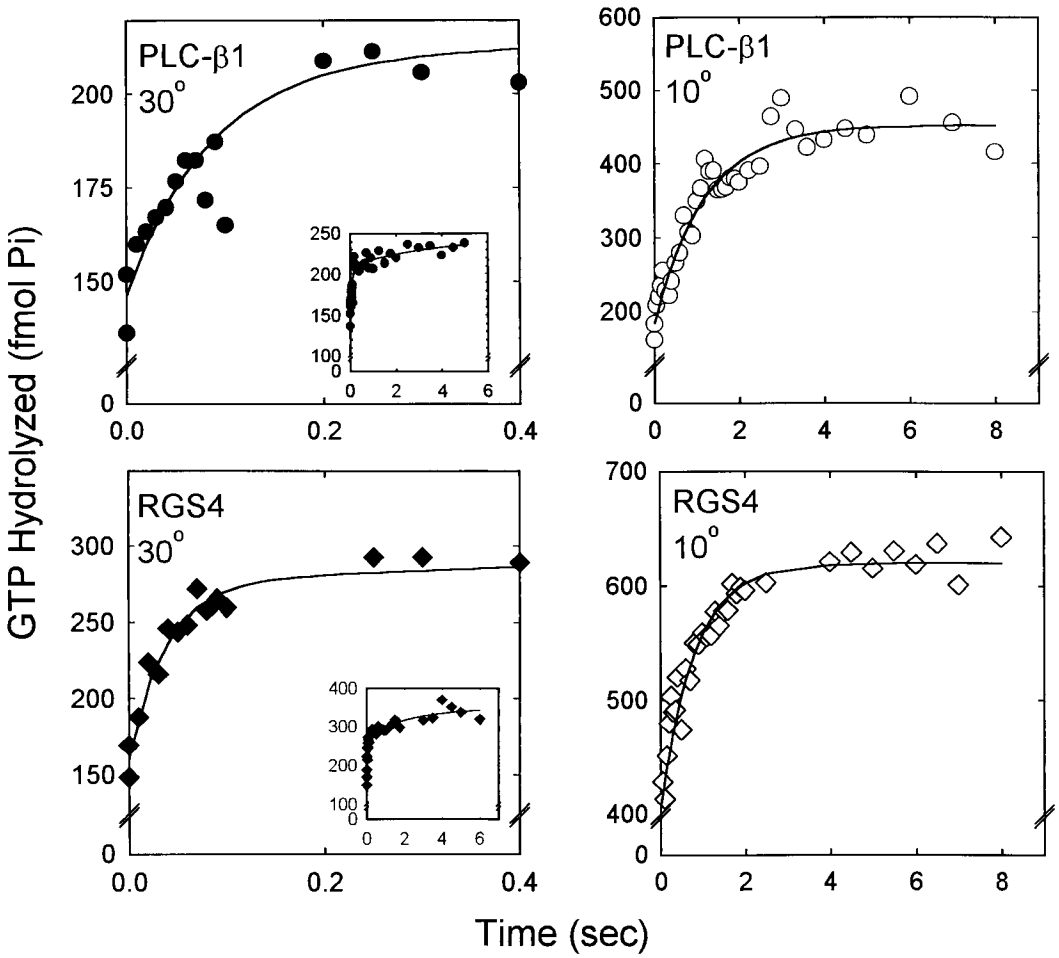

FIG. 3. GAP-stimulated hydrolysis of G_q-bound GTP. m1AChR-G_q vesicles and either 44 nM PLC or 9 μM RGS4 were incubated with 1 mM carbachol for at least 15 min at 10°C or 3 min at 30°C. Aliquots were then diluted 1:2 with carbachol and [γ-^{32}P]GTP (300–700 nM) and allowed to incubate for 1 min at 10°C or 6 s at 30°C. At $t = 0$, this mixture was diluted 1:1.5 further with buffer that contained unlabeled GTP and atropine and incubated for the times shown. Solid lines are fits to first-order rate equations to yield the following rate constants (k_{hydrol}): PLC-β1, 30°C, 11.9 s^{-1}; PLC-β1, 10°C, 0.84 s^{-1}; RGS4, 30°C, 27 s^{-1}; RGS4, 10°C, 1.2 s^{-1}. Data obtained at 30°C are fit to two components, that listed above and a slower one visible in the insets (see *Results*). Vesicles contained the following amounts of receptor and G_q, in the above order: 68 fmol and 187 fmol; 106 fmol and 260 fmol; 106 fmol and 260 fmol; and 150 fmol and 432 fmol. Each data set is representative of at least two experiments using different m1AChR-G_q vesicle preparations.

(Fig. 2), although we were unable to demonstrate saturation because of assay background at high [γ-^{32}P]GTP concentrations. At 30°C, the burst was followed by a second slower phase of GTP hydrolysis with an apparent rate constant of $\approx$0.35 s^{-1} (Fig. 3 *Insets*). This is about equivalent to rates observed in vesicles that contained too low a m1AChR/G_q ratio to display a measurable burst. We interpret this slower second phase to represent a combination of receptor-promoted binding of GTP to G_q and subsequent hydrolysis. We have not pursued it further.

GDP Dissociation. Because hydrolysis of G_q-bound GTP was found to be so fast, we reexamined the activating steps of the GTPase cycle, GDP release, and GTP binding. To measure the dissociation of GDP from G_q, we allowed [α-^{32}P]GDP to bind G_q in a syringe of the quench-flow mixer by incubating m1AChR vesicles either with agonist and [α-^{32}P]GDP itself or with agonist, GAP, and [α-^{32}P]GTP. We then diluted the mixture into excess unlabeled GTP and, after appropriate times, quenched the mixture and measured remaining bound [α-^{32}P]GDP (Fig. 4). The average GDP dissociation rate constant k_{diss} was 1.5 s^{-1} at 30°C (1.8 s^{-1} maximum), about 4-fold faster than estimated previously by using manual mixing (18). This value was consistently somewhat higher than k_{cat} (V_{max}/[E]) for the steady-state GTPase reaction (Figs. 1 and 2), suggesting that receptor-promoted dissociation of GDP is the principal rate-limiting step in the GTPase cycle when GAP, agonist, and GTP are all present at saturating concentrations. The value of k_{diss} did not vary whether [α-^{32}P]GDP itself was bound to G_q in the absence of a GAP or it was generated on G_q in the presence of either PLC-β1 or RGS4 (data not shown). At 10°C, k_{diss} was 0.14 s^{-1}, also in agreement with k_{cat} at that temperature (Figs. 1 and 2). The amount of [α-^{32}P]GDP released was appropriate for the amount of G_q in the reaction mixture and its fractional saturation. Dissociation was monophasic at 10°C, but a small, very slow second phase could be detected at 30°C. Neither the rate nor magnitude of the slow phase could be measured accurately. GDP dissociation was independent of the concentration of free GTP present during the dissociation reaction (data not shown).

Receptor-Catalyzed GDP/GTP Exchange. Because receptor-promoted dissociation of GDP from G_q appeared to be rate-limiting at high GTP concentrations and was much smaller than k_{hydrol}, we measured the rate of GDP/GTP exchange, a combination of GDP release and GTP binding, to test the role of GTP binding to nucleotide-free G_q in the GTPase cycle. Vesicles, with or without a GAP, were incubated with agonist and then mixed with radiolabeled nucleotide, either [α-^{32}P]GTP or [^{35}S]GTPγS. Exchange reactions

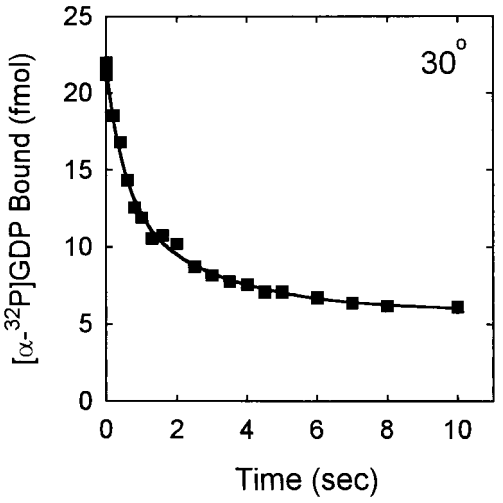

FIG. 4. Receptor-stimulated GDP dissociation. m1AChR-G_q vesicles were incubated with 300 nM [α-^{32}P]GDP and 1 mM carbachol for at least 3 min at 30°C. Aliquots (10 fmol m1AChR, 26 fmol G_q) were then diluted 1:2 with 500 μM nonradioactive GTP and 1 mM carbachol. Mixtures were quenched at the times shown. Bound [α-^{32}P]GDP was determined by nitrocellulose filter binding. The solid line represents a fit to a bi-exponential function with a principal dissociation rate constant k_{diss} of 1.84 s^{-1} (55% of total) and a slower component (0.35 s^{-1}). Data are from one of five different experiments that yielded similar fast (1.6 s^{-1} mean) and slow (0.21 s^{-1} mean) dissociation rates.

were quenched at appropriate times, and the accumulation of bound nucleotide was fit to first-order rate equations to yield the rate constant, k_{exch} (Fig. 5 *Upper*). Binding of [α-^{32}P]GTP and [^{35}S]GTPγS yielded similar exchange rates over a relatively wide concentration range, and these rates were unaltered by the presence of either PLC-β1 or RGS4 (Fig. 5 *Lower*). Thus, neither GAP acts as an exchange catalyst regardless of whether the nucleotide bound can be hydrolyzed.

GDP/GTP exchange was relatively slow over the range of GTP concentrations studied, with k_{exch} significantly below k_{diss}. Although we were not able to demonstrate saturation of k_{exch}, its value depended on the concentration of free nucleotide in a pattern similar to the rate of the overall GTPase cycle, with k_{exch} approximately equal to the molar turnover number over the accessible range of GTP concentrations (compare Figs. 5 *Lower* and 2). At saturating GTP (Fig. 2), $k_{cat} \approx k_{diss}$ for GDP. The rate of GTP binding to G_q, itself limited by GDP dissociation, thus appears to be rate-limiting for the GTPase reaction at all concentrations of GTP.

Because k_{diss} is not altered by the concentration of free nucleotide, the observed dependence of k_{exch} on the GTP concentration reflects rate-limiting GTP binding at these concentrations (Fig. 5). This idea is corroborated by the observation that allowing G_q to bind either IDP or XDP before the assay did not alter k_{exch} (data not shown), even though these nucleotides bind $G\alpha_q$ with much lower affinity than does GDP and also dissociate much faster (22). We can therefore use the dependence of k_{exch} on GTP concentration to determine the rate constant, k_{assoc}, for GTP binding to nucleotide-free G_q from k_{exch} to be $\approx 1 \times 10^5$ $M^{-1}\cdot s^{-1}$ at 30°C. [A plot of k_{exch} vs. the concentration of GTP is a line with slope 1×10^5 $s^{-1}\cdot M^{-1}$. Because k_{diss} is much greater than the measured values of k_{exch} over this range of GTP concentrations, this slope approximates $k_{assoc,\ GTP}$.] Based on this value, increasing the concentration of GTP should increase k_{exch} until it surpasses k_{diss} for GDP, 1.5 s^{-1}, at about 15 μM GTP. Thus, GTPase activity reaches saturation at high GTP concentrations when GDP dissociation becomes rate-limiting.

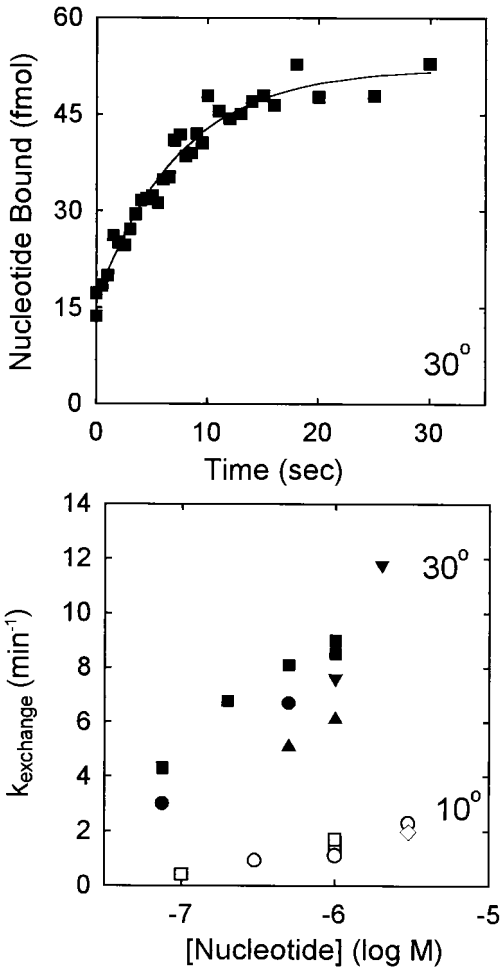

FIG. 5. Receptor-stimulated guanine nucleotide exchange. (*Upper*) Time course of binding of GTPγS to m1AChR-G_q vesicles. m1AChR-G_q proteoliposomes and 1 mM carbachol were incubated at 30°C for at least 3 min. Aliquots (12 fmol m1AChR, 47 fmol G_q) were diluted 1:2 with 500 nM [^{35}S]GTPγS for the times shown before quenching and measurement of bound [^{35}S]GTPγS. The solid line shows a fit to a first-order rate equation with $k_{exch} = 0.135\ s^{-1}$. (*Lower*) Dependence of exchange rates on the concentration of free nucleotide. Nucleotide exchange was measured as described above in the presence of increasing concentrations of radiolabeled nucleotide at either 30°C (solid symbols) or 10°C (open symbols). Values of k_{exch} are plotted vs. the concentration of free nucleotide. At 10°C, exchange was relatively slow and was measured manually by using a protocol identical to that described for the quench-flow mixer except that the preincubation time was at least 15 min. Labeled nucleotides were [^{35}S]GTPγS in the presence of either 15 nM PLC-β1 (●, ○) or 4 μM RGS4 (◇) or without GAP (■, □), or [α-^{32}P]GTP with PLC-β1 present (▲) or absent (▼).

DISCUSSION

G protein GAPs allow rapid termination of a signal on removal of agonist, but can also substantially inhibit signaling in the presence of agonist by shortening the activation lifetime of the G protein during the GTPase cycle. The data presented here describe how the individual steps in the GTPase cycle combine to produce both robust activation by agonist and rapid deactivation on agonist removal. Such balance is particularly important for G protein-regulated effectors, such as PLC-β1, that use intrinsic GAP activity to modulate the kinetics of their own activation.

The most striking outcome of this study was the speed of GAP-stimulated hydrolysis of G_q-bound GTP, with an average k_{hydrol} of 25 s^{-1} for RGS4 and 15 s^{-1} for the effector PLC-β1 at 30°C. This represents a 2,000-fold increase over the basal

rate of 0.013 s^{-1} (12), comparable to the 10,000-fold effect of ras GAP on p21ras (23). Moreover, G protein GAPs accelerate GTP hydrolysis by an allosteric mechanism, whereas GAPs for small monomeric GTP-binding proteins provide a catalytic arginine residue to the active site in addition to any conformational influence (24).

The GTP hydrolysis rates determined here agree well with cellular rates of signal termination on removal of agonist. PLC-β1-stimulated hydrolysis occurred with a half-time of 50–75 ms at 30°C, commensurate with that for closure of G$\beta\gamma$-regulated K^+ channels (4, 8) or for termination of the G_q-mediated photoresponse in *Drosophila* (25). Although we did not measure k_{hydrol} at 37°C, extrapolation from the values at 10°C and 30°C suggest that the PLC-β1-stimulated turn-off rate at 37°C will be about 25 s^{-1}, a deactivation half-time of about 25 ms, and thus accounts well for physiological turn-off rates without recourse to other desensitizing mechanisms.

Both the maximal rate of GAP-stimulated hydrolysis of G_q-bound GTP observed here, 27 s^{-1}, and the relative stimulation above the basal rate are notably greater than those described previously for heterotrimeric G protein GAPs, even though basal k_{hydrol} for Gα_q is only about 25% that for G_i, G_o, or G_s (12). For comparison, members of the G_z GAP subfamily of RGS proteins (RGSZ1, GAIP, RET-RGS1) elevated k_{hydrol} about 400-fold for G_z in solution (26). Arshavsky *et al.* (27) reported that RGS4-stimulated G_t hydrolyzed GTP at a rate of 2.8 s^{-1} at 22°C, and Posner (28) reported a rate of 2.0 s^{-1} for soluble RGS4-stimulated G_o at 8°C. The vesicle system used here may contribute to the high GAP activities that we observed. Effects of both PLC-β1 and RGS4 on G_q were much larger here than in a study of detergent-solubilized RGS4 and a mutant Gα_q (29), and the GAP activities of RGS2 and several RGS4 mutants are greater in vesicles than in detergent solution (28, 30).

The rates determined here for receptor-promoted GDP dissociation and overall GDP/GTP exchange, k_{diss} and k_{exch}, are also significantly faster than previously determined for purified receptors and G proteins. More importantly, k_{exch} is adequate to activate G_q substantially despite rapid GTP hydrolysis. Based on the values of k_{hydrol} and k_{exch}, m1AChR can maintain ≈15% of total G_q in the activated state in the presence of saturating agonist and PLC-β1. [The fraction of G_q activated at steady-state is equal to $k_{exch}/(k_{exch} + k_{hydrol})$]. Presumably, a cell can do somewhat better, but even cellular signaling systems are typically much more active in the presence of nonhydrolyzable GTP analogs than with GTP itself. Although it is not feasible to measure these individual reactions in intact cells or native cell membranes, the values reported here should approximate physiological parameters reasonably well.

Two considerations indicate that the GDP/GTP exchange rate is the principal rate-limiting step in the GTPase cycle in the presence of both agonist and GAP. First, the steady-state turnover number is only slightly greater than k_{exch} over the range of GTP concentrations where it could be measured. In addition, the maximum steady-state rate (k_{cat}) saturates at a value approximately equal to the experimentally determined value of k_{diss}, which is necessarily the upper limit of k_{exch}. Although we could not directly measure the second-order rate constant for GTP binding to the complex of receptor and unliganded G_q, its calculated value is 1×10^5 $s^{-1} \cdot M^{-1}$. At cellular concentrations of GTP (200–500 μM) (31), the rate of binding of GTP to unliganded G_q would substantially exceed the rate of GDP dissociation, and dissociation from the receptor–G protein complex will be the essentially rate-limiting step for GDP/GTP exchange. Thus, the rate of activation of G_q and its level of steady-state activation will be determined by how quickly the receptor drives GDP dissociation. We propose that the two principal determinants of receptor's efficacy will be the value of k_{diss} that it can achieve and the stability of its binding to G protein during multiple turnovers of the GTPase cycle.

We thank Karen Chapman for expert and careful technical assistance throughout this study and Harold Brooks, Gloria Biddlecome, and Yves Dupont for discussion and suggestions. This work was supported by National Institutes of Health Grants GM30355 and CA66187 and by R. A. Welch Foundation Grant I-0982.

1. Dohlman, H. G., Song, J. P., Ma, D. R., Courchesne, W. E. & Thorner, J. (1996) *Mol. Cell. Biol.* **16,** 5194–5209.
2. Koelle, M. R. & Horvitz, H. R. (1996) *Cell* **84,** 115–125.
3. Wieser, J., Yu, J.-H. & Adams, T. H. (1997) *Curr. Genet.* **32,** 218–224.
4. Zerangue, N. & Jan, L. Y. (1998) *Curr. Biol.* **8,** 313–316.
5. Dohlman, H. G. & Thorner, J. (1997) *J. Biol. Chem.* **272,** 3871–3874.
6. Berman, D. M. & Gilman, A. G. (1998) *J. Biol. Chem.* **273,** 1269–1272.
7. Arshavsky, V. Y. & Pugh, E. N., Jr. (1998) *Neuron* **20,** 11–14.
8. Doupnik, C. A., Davidson, N., Lester, H. A. & Kofuji, P. (1997) *Proc. Natl. Acad. Sci. USA* **94,** 10461–10466.
9. Saitoh, O., Kubo, Y., Miyatani, Y., Asano, T. & Nakata, H. (1997) *Nature (London)* **390,** 525–529.
10. Chuang, H.-H., Yu, M., Jan, Y. N. & Jan, L. Y. (1998) *Proc. Natl. Acad. Sci. USA* **95,** 11727–11732.
11. Bünemann, M. & Hosey, M. M. (1998) *J. Biol. Chem.* **273,** 31186–31190.
12. Berstein, G., Blank, J. L., Jhon, D.-Y., Exton, J. H., Rhee, S. G. & Ross, E. M. (1992) *Cell* **70,** 411–418.
13. Hart, M. J., Jiang, X., Kozasa, T., Roscoe, W., Singer, W. D., Gilman, A. G., Sternweis, P. C. & Bollag, G. (1998) *Science* **280,** 2112–2114.
14. Kozasa, T., Jiang, X., Hart, M. J., Sternweis, P. M., Singer, W. D., Gilman, A. G., Bollag, G. & Sternweis, P. C. (1998) *Science* **280,** 2109–2111.
15. Scholich, K., Mullenix, J. B., Wittpoth, C., Poppleton, H. M., Pierre, S. C., Lindorfer, M. A., Garrison, J. C. & Patel, T. B. (1999) *Science* **283,** 1328–1331.
16. Breitwieser, G. E. & Szabo, G. (1988) *J. Gen. Physiol.* **91,** 469–493.
17. He, W., Cowan, C. W. & Wensel, T. G. (1998) *Neuron* **20,** 95–102.
18. Biddlecome, G. H., Berstein, G. & Ross, E. M. (1996) *J. Biol. Chem.* **271,** 7999–8007.
19. Berstein, G., Blank, J. L., Smrcka, A. V., Higashijima, T., Sternweis, P. C., Exton, J. H. & Ross, E. M. (1992) *J. Biol. Chem.* **267,** 8081–8088.
20. Berman, D. M., Wilkie, T. M. & Gilman, A. G. (1996) *Cell* **86,** 445–452.
21. Brandt, D. R. & Ross, E. M. (1986) *J. Biol. Chem.* **261,** 1656–1664.
22. Chidiac, P., Markin, V. S. & Ross, E. M. (1999) *Biochem. Pharmacol.* **58,** 39–48.
23. Gideon, P., John, J., Frech, M., Lautwein, A., Clark, R., Scheffler, J. E. & Wittinghofer, A. (1992) *Mol. Cell. Biol.* **12,** 2050–2056.
24. Scheffzek, K., Ahmadian, M. R., Kabsch, W., Wiesmüller, L., Lautwein, A., Schmitz, F. & Wittinghofer, A. (1998) *Science* **277,** 333–338.
25. Ranganathan, R., Harris, G. L., Stevens, C. F. & Zuker, C. S. (1991) *Nature (London)* **354,** 230–232.
26. Wang, J., Ducret, A., Tu, Y., Kozasa, T., Aebersold, R. & Ross, E. M. (1998) *J. Biol. Chem.* **273,** 26014–26025.
27. Nekrasova, E. R., Berman, D. M., Rustandi, R. R., Hamm, H. E., Gilman, A. G. & Arshavsky, V. Y. (1997) *Biochemistry* **36,** 7638–7643.
28. Posner, B. A., Mukhopadhyay, S., Tesmer, J. J., Gilman, A. G. & Ross, E. M. (1999) *Biochemistry* **38,** 7773–7779.
29. Chidiac, P. & Ross, E. M. (1999) *J. Biol. Chem.* **274,** 19639–19643.
30. Ingi, T., Krumins, A. M., Chidiac, P., Brothers, G. M., Chung, S., Snow, B. E., Barnes, C. A., Lanahan, A. A., Siderovski, D. P., Ross, E. M., *et al.* (1998) *J. Neurosci.* **18,** 7178–7188.
31. Traut, T. W. (1994) *Mol. Cell. Biochem.* **140,** 1–22.